Journal of Applied Mechanics and Technical Physics, Vol. 41, No. 3, 2000

EXPERIMENTAL STUDY OF DENSITY FLUCTUATIONS IN A HYPERSONIC LAMINAR WAKE BEHIND A CONE

V. M. Aniskin and S. G. Mironov

UDC 532.526.013.4+533.6.011.5

The characteristics of natural fluctuations of density in a laminar near wake behind a sharp cone in a hypersonic flow of nitrogen at zero incidence are studied by the method of electron-beam fluorescence at Mach number $M = 21$ *and unit Reynolds number* $Re_1 = 6 \cdot 10^5$ m^{-1}. *The distributions of the mean density, integral fluctuations, and spectra of density fluctuations are obtained, the longitudinal and azimuthal phase velocities of perturbations are determined, and the growth rates of perturbations in the wake are found. The results are compared with the measurement data in the shock layer on a flat plate.*

Much attention is given to aerodynamics of hypersonic boundary layers and hypersonic mixing layers. One important problem is the study of perturbations in aerodynamic wakes behind bodies. The results of these studies are very important for understanding the mechanisms of the laminar–turbulent transition in shear flows and are used to develop the combustor duct of a hypersonic air-breathing engine and to design aerodynamic control elements of hypersonic flying vehicles.

Only some scattered experimental studies are currently available on aerodynamic characteristics and flow stability in the wake behind the bodies in a hypersonic flow, in particular, behind cones [1–4]. The data in these works refer mainly to the mean parameters of the wake flow and are obtained for high Reynolds numbers and moderate hypersonic Mach numbers. The wake field behind a cone for high Mach numbers and moderate Reynolds numbers was studied only by Allegre and Raffin [2]. There are no data on evolution and local characteristics of perturbations in [1–4].

At the same time, there are theoretical papers on the stability of hypersonic laminar mixing layers to which wake flows refer (see, for example, [5]). The mean flow parameters used for stability modeling are simple and correspond to the far wake in which the spatial distributions of the parameters are self-similar. The flow pattern in the near wake is much more complicated, since there are large crossflow and streamwise gradients of parameters there. The near wake retains information about the disturbance field of the boundary layer on the body, which makes theoretical study more difficult. Nevertheless, it is in the near wake that the initial disturbances developing downstream are formed, which stipulates the necessity of studying the near-wake stability.

The objective of the present study is to obtain a full set of the characteristics of density perturbations in a laminar near wake behind a cone in a hypersonic nitrogen flow at Mach number $M = 21$ and unit Reynolds number $Re_1 = 6 \cdot 10^5$ m^{-1}.

1. Experimental Equipment. The experiments were conducted in the T-327A hypersonic nitrogen wind tunnel of the Institute of Theoretical and Applied Mechanics of the Siberian Division of the Russian Academy of Sciences [6] with a conical nozzle designed for an exit Mach number $M = 20$. The streamwise gradient of the Mach number in the test section was 3 m^{-1}, and the integral level of density fluctuations

Institute of Theoretical and Applied Mechanics, Siberian Division, Russian Academy of Sciences, Novosibirsk 630090. Translated from Prikladnaya Mekhanika i Tekhnicheskaya Fizika, Vol. 41, No. 3, pp. 111–117, May–June, 2000. Original article submitted July 26, 1999.

in the flow core was less than 0.5%. In our experiments, the stagnation pressure P_0 was 8 MPa, and the stagnation temperature was sustained at a level of 1100 K to avoid nitrogen condensation. For these conditions, the density (concentration) of nitrogen molecules n_∞ in the region of measurements in the free flow was $6.8 \cdot 10^{21}$ m^{-3}. The experimental facility had an electron gun to generate a probing electron beam [7].

An aluminum cone was used as a model in our experiments. The cone length was 0.113 m, the base diameter was 0.04 m, and the apex half-angle was 10°. The bluntness radius of the cone tip was less than 0.05 mm, i.e., it was of the order of the mean free path of the molecules. The cone was mounted at zero angle of attack.

The sting of the model fixed at the cone base was attached to a traversing gear, which allowed streamwise displacement of the model at a distance up to 0.2 m. This displacement allowed us to scan the wake field for different values of the X coordinate, but the Mach number at the flow/cone tip interaction point varied from 20.0 to 20.8. The traversing gear together with the model could move across the flow (in the Y direction) at a distance up to 0.1 m.

The mean density and density fluctuations in the near wake behind the cone were measured by the method of electron-beam fluorescence within the range of distances from the cone base $X/d = 0.75$–6 (d is the cone-base diameter). In the experiments, the electron beam was stationary and crossed the flow in a region where the local Mach number was $\mathrm{M} = 21$. The optical system of registration of nitrogen fluorescence and the technique for signal processing for obtaining the mean and fluctuating characteristics of density in the flow are described in detail in [7, 8]. The optical axis of the registration system was directed along the Y axis. The optical system had a traversing gear for scanning nitrogen fluorescence along the electron beam, which ensured measurements for different values of the Z coordinate. The field of the mean density and density fluctuations was measured in a plane passing through the wake centerline perpendicular to the optical axis. The electron beam crossed the wake over its diameter, and the Z coordinate was actually the radial coordinate.

The measurement technique of the longitudinal and azimuthal phase velocity is also described in [7, 8]. The phase velocities of the disturbances were measured in the regions of the maximum of the radial distribution of the integral density fluctuations in the wake. The streamwise phase velocity was measured by moving the fluorescence-registration points apart by a distance of 0.023 m in the XY plane (phase-measurement base) along the wake axis. In measurements of the azimuthal phase velocity, the model was shifted toward the Y axis (in the direction of the optical axis of the registration system), and the electron beam crossed the cylindrical region of maximum fluctuations along the chord 0.023 m long. The registration points of the optical system were placed with the same gap along the electron beam.

Relations for calculating the dimensionless frequency parameter F, the growth rate of density fluctuations α_i, the longitudinal and azimuthal phase velocities C_x and C_φ, and the angle of propagation of density waves χ are similar to those given in [7, 8].

2. Technique of Determination of the Mean Density and Density Fluctuations. As compared to the case of the flat-plate flow, the flow in a hypersonic wake behind a cone has some special features, which facilitate the problem of electron-beam diagnostics. Since the gas density in the wake behind the cone and in the free stream outside the shock-wave region is considerably lower than the density in the shock wave, no significant scattering of electrons occurs here. The major scattering of the electron beam occurs in the shock-wave region. Attenuation of the electron beam in the external flow can be avoided by normalizing the mean-density signal to its value immediately ahead of the shock wave. This is allowable since the density distribution in the external flow is assumed to be uniform. If the fluorescence intensity is measured along the electron beam that passes along the wake diameter, we can expect a considerably smaller scattering of the electron beam on the shock wave as compared to the measurements of [7, 8], where the beam penetrates through the flow along the shock-wave plane at a significant distance (about 0.05 m). In this case, the integral scattering of the beam is rather small, and we can use only the values of the local density at the measurement point.

This fact allows us to consider the process of collisional quenching of electron excitation of the molecules as the basic one. As a function of fluorescence-intensity attenuation, we can use the Stern–Volmer dependence, from which we obtain

$$\frac{n}{n_\infty} = \frac{I/I_\infty}{1 - K_\tau(I/I_\infty)}. \tag{1}$$

Here n/n_∞ and I/I_∞ are the gas density and the mean signal of the optical system normalized to the corresponding free-stream values and K_τ is a quenching constant, which takes into account collisional deactivation of molecules determined from the data of Belikov [9] for the gas temperature behind the shock wave. This choice of temperature is due to the fact that the density is maximum immediately behind the shock wave, and hence, the effect of collisional deactivation is also maximum. Ahead of and behind the shock wave, the density dramatically decreases, and the effect of this process becomes significantly weaker. A similar approach was used by Harbour and Lewis [10] for measuring the mean-density distribution in the shock layer on a flat plate under test conditions close to those of the present work. Formula (1) was used to reconstruct the mean density distribution in the wake. The gas temperature behind the shock wave was determined from the relations for the shock adiabat taking into account the actual value of the shock-wave inclination to the flow direction. The angle of inclination was found from photographs of electron-beam visualization of the flow field.

Nevertheless, the accuracy of density reconstruction in the wake can be improved by taking into account the scattering of electrons in the gas. Assuming that the dependence of attenuation of the probing beam in the gas is exponential and using the data on signal variation along the beam at the sector of its intersection with the external flow, we can determine the effective coefficient of attenuation β. This coefficient is equal to (6.0 ± 0.2) m^{-1}. After that, the actual value of density at the point z was found by iterations using the relation

$$\Big(\frac{n}{n_\infty}\Big)_{N+1} = \Big(\frac{n}{n_\infty}\Big)_0 \Big/ \exp\Big[-\beta\int_a^z \Big(\frac{n}{n_\infty}\Big)_N dl\Big] \qquad (N = 0, 1, 2, \ldots).$$

Here $(n/n_\infty)_0$ is the value at the point z obtained from (1), a is the value of the Z coordinate ahead of the shock wave, l is the distance along the beam from the point a to the point z, and N is the number of iterations. The calculations show that $n/n_\infty(z)$ converges to a finite value already after two iterations.

Because of measurement locality, the relationship between the normalized density fluctuations n'/n_∞ at the measurement point and the normalized variable of the output signal component I'/I_∞ is determined by a derivative from relation (1):

$$\frac{n'}{n_\infty} = \frac{I'}{I_\infty}\Big(1 + K_\tau\frac{n}{n_\infty}\Big)^2.$$

It follows from here that the magnitude of density fluctuations depends not only on the value of the variable component of the signal but also on the mean value of density at the measurement point.

3. Measurement Results. Figure 1 shows the radial distribution of the spectra of density fluctuations in the cross section $X/d = 1$. The distribution is plotted as isolines of the logarithm of the fluctuation amplitude. The spectra are normalized to one value of the amplitude for frequencies above $2.5 \cdot 10^{-4}$. The logarithmic representation of the amplitude and normalization of the spectra allow one to exclude the influence of the amplitude dependence on the local mean density on the spectrum shape and to reveal actual changes in the frequency distribution of the fluctuation intensity. It is seen from Fig. 1 that the share of low-frequency fluctuations increases significantly in the shock-wave region. Behind the shock wave, high-frequency disturbances prevail in the spectrum. The qualitative character of the frequency distribution of fluctuations is identical in the entire wake region examined.

Figure 2 shows the spectra of the phase velocities in the longitudinal C_x (points 1 for the cross section $X/d = 2.3$) and azimuthal C_φ directions (points 2 for the cross section $X/d = 1.5$ and points 3 for $X/d = 4$). The abscissa axis for phase velocities at the top of Fig. 2 shows the dimensionless frequency of density fluctuations F. The frequency parameter F was determined in [8]. Figure 2 shows the approximation dependences with intervals characterizing the error in determining phase velocities. For curve 3, only the lower limits of deviation are given.

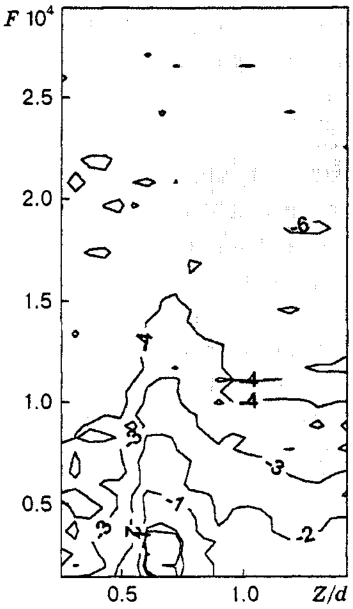

Fig. 1

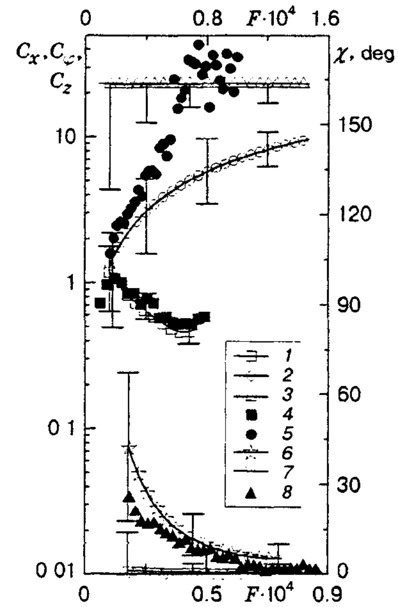

Fig. 2

Figure 2 shows also the data for a flow past a flat plate [8] (points 4 correspond to C_x and points 5 to C_z). The streamwise phase velocity C_x of perturbations propagating in the wake does not depend on the X coordinate within the measurement accuracy and is close to the streamwise phase velocity in the shock layer on a flat plate. The dependence of the azimuthal phase velocity of perturbations on the frequency parameter $C_\varphi(F)$ for the cross section $X/d = 1.5$ is in qualitative agreement with the frequency dependence for the spanwise phase velocity $C_z(F)$ on a flat plate, but the quantitative disagreement increases with increasing frequency. Possibly, this depends on the type of two-dimensional flow (axisymmetric or plane).

It is also seen from Fig. 2 that the azimuthal phase velocity in the cross section $X/d = 4$ (points 3) is much greater than the phase velocity in the cross section $X/d = 1.5$ (points 2). On the basis of the spectra of the longitudinal and azimuthal phase velocity for these cross sections, we calculated the spectra of the angles of inclination of the wave vector to the flow axis χ (in degrees). Points 6 in Fig. 2 correspond to the cross section $X/d = 1.5$ and points 7 to $X/d = 4$. The abscissa axis for the angular dependences is given at the bottom of Fig. 2. Points 8 in Fig. 2 correspond to the spectrum of the angles χ obtained for a flat plate [8]. The dependences for the cross section $X/d = 1.5$ are similar. The decrease in inclination of the wave vector to the flow axis indicates an increase in the share of two-dimensional waves in the wake with increasing distance from the cone base. One of the possible reasons for that is the flow divergence whose effect was observed in measurements in a moderately hypersonic boundary layer on a cone. The initiation of inclined waves in the wake behind a cone, as in the shock layer on a flat plate, may be connected with the existence of strongly inclined waves in the free stream [8]. The values of the streamwise phase velocity smaller than $1 - 1/\mathrm{M}_e = 0.88$ (M_e is the Mach number behind the shock wave) indicate an acoustic nature of perturbations, at least for the frequency parameter F higher than $0.2 \cdot 10^{-4}$. This value distinguishes vortex-mode perturbations from acoustic-mode perturbations in the linear theory of stability of compressible flows [11].

Figure 3a shows the isolines of normalized density in the axial section of the wake behind a cone. The bow shock wave is clearly seen in the form of a straight-line sharp ridge transforming into a plateau on the internal slope of the distribution with distance from the cone base. Its formation is related to gradual liberation of a mixing layer from the shock layer.

In calculating the growth rate of density fluctuations in the wake, the main difficulty is the absence of a clearly expressed line of the maximum of integral density fluctuations of the mixing layer similar to

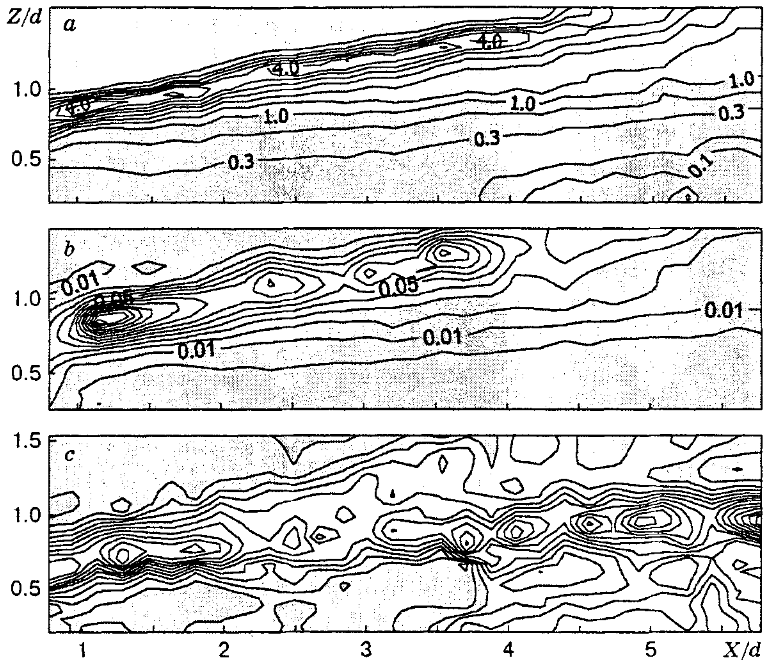

Fig. 3

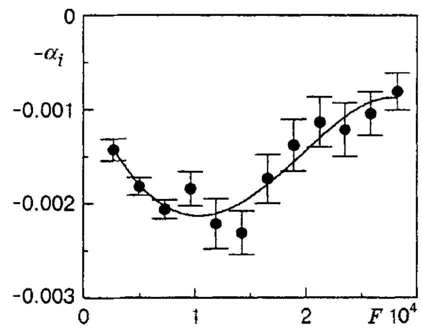

Fig. 4

that along which the growth rate of fluctuations was calculated for the flow past a flat plate [8, 12]. It is shown [12] that the spectrum of the growth rate of perturbations depends significantly on the trajectory along which the measurements are performed. Figure 3b shows the isolines of the field of normalized integral density fluctuations in the wake. The density fluctuations are concentrated mainly in the vicinity of the shock wave. This may be related to shock-wave oscillations under the action of perturbations of the external flow; therefore, we had to first find the position of the maximum of density fluctuations associated with the flow in the shear layer under the shock wave. It was assumed that the fluctuations in the wake consist of two components: fluctuations of the density shock and fluctuations related to evolution of instability of the shear layer. Since the density in the shock wave varies weakly along the wake, the value of density fluctuations induced by shock-wave oscillations should be proportional to the mean density. This allows us to identify fluctuations related to the shear layer by dividing the values of integral fluctuations by the mean density at each point. This procedure does not allow one to obtain the actual values of density fluctuations related to evolution of instability but makes it possible to identify (visualize) their position in the wake, since the first component of fluctuations degenerates into a rather uniform background (Fig. 3c).

The dependence $Z(X)$ of the positions of the maximums in Fig. 3c is approximated by a power-law function with an exponent equal to 0.44 (X is calculated from the cone tip). This dependence is close to the dependence $Z = X^{1/2}$ typical of a laminar mixing layer. The spectrum of the growth rates of density fluctuations $\alpha_i(F)$ is calculated along the lines of the positions of the maximums; it is plotted in Fig. 4. The growth rates are calculated for the interval 0.03–0.23 m from the cone base. Figure 4 also shows the values of the credibility interval. Decay of fluctuations at all frequencies can be noted. Perturbations at high frequencies decay less intensively than at low frequencies. This agrees with the measurement results of fluctuation spectra plotted in Fig. 1, which shows the prevailing of high-frequency perturbations in the wake. It is shown experimentally that gas acceleration at the wake axis is observed at distances from the cone base up to $X/d = 6$ [2]. This indicates the presence of a negative pressure gradient in the wake. The latter may be the reason for stabilization of the shear layer and suppression of the growth of perturbations observed in experiment.

Conclusions. A measurement technique for the mean density and density fluctuations has been developed for axisymmetric hypersonic wake flows on the basis of electron-beam fluorescence of nitrogen. The mean-density field and the characteristics of perturbations in a hypersonic near wake behind a sharp cone with a half-angle of 10° have been measured for the first time for a flow Mach number $\mathrm{M} = 21$ and unit Reynolds number $\mathrm{Re}_1 = 6 \cdot 10^5$ m. It is shown that inclined waves are developed in the wake behind the cone, and the angle of inclination of these waves decreases with distance from the cone base. The longitudinal phase velocity of these waves is close to the streamwise phase velocity of density waves on the surface of a flat plate. It has been shown experimentally that the angles of inclination of the wave vector to the flow axis in the wake and on a flat plate coincide. Spectra of the growth rate of density fluctuations corresponding to a decaying wave process have been obtained, which can be attributed to the stabilizing effect of the negative pressure gradient and flow acceleration in the near wake.

REFERENCES

1. S. Yu. Chernyavskii, "Wake dimensions behind a cone flying with a hypersonic velocity," *Izv. Akad. Nauk SSSR, Mekh. Zhidk. Gaza*, No. 6, 76–78 (1976).
2. J. Allegre and M. Raffin, "Flow determination along a wake axis," in: *Proc. of the 9th Int. Symp. on Rarefied Gas Dynamics*, Vol. 1, Göttingen (1974), pp. B9.1–B9.11.
3. Z. Levensteins and M. Krumins, "Aerodynamic characteristics of hypersonic wakes," *Raket. Kosm. Tekh.*, **5**, No. 9, 31–42 (1967).
4. M. J. Marcillat, "Configuration du sillage proche hypersonique d'un cone circulaire elance," *C. R. Acad. Sci., Paris, Sér. A*, **269**, 1217–1220 (1969).
5. D. T. Papageorgiou, "The stability of two-dimensional wakes and shear layers at high Mach numbers," *Phys. Fluids A*, **3**, No. 5, 793–802 (1991).
6. I. G. Druker, V. D. Zhak, B. A. Sapogov, and Yu. A. Safronov, "Characteristics of a hypersonic nitrogen wind tunnel of the Institute of Theoretical and Applied Mechanics, Siberian Division, USSR Academy of Sciences," in: *Problems of Gas Dynamics* (collected scientific papers), Inst. of Theor. and Appl. Mech., Sib. Div., USSR Acad. of Sci., No. 5, 294, 295 (1975).
7. A. A. Maslov and S. G. Mironov, "Electron-beam diagnostics of hypersonic flows," *Exp. Measur. Fluid Mech.*, **12**, No. 4, 42–52 (1998).
8. A. A. Maslov, S. G. Mironov, and A. N. Shiplyuk, "Wave processes in a hypersonic shock layer on a flat plate," *Izv. Ross. Akad. Nauk, Mekh. Zhidk. Gaza*, No. 5, 162–168 (1998).
9. A. E. Belikov, "Rate constants of molecular energy-exchange reactions at low temperatures," Doctoral Dissertation in Phys.-Math. Sci., Novosibirsk (1996).
10. P. J. Harbour and J. H. Lewis, "Preliminary measurements of the hypersonic rarefied flow field on a sharp plate using an electron beam probe," in: C. L. Brundin (ed.), *Rarefied Gas Dynamics*, Academic Press, New York (1967), pp. 1031–1046.
11. L. M. Mack, *Boundary Layer Stability Theory* (Rev. A, Doc. 900–277), JPL, Pasadena, CA (1969).
12. A. A. Maslov and S. G. Mironov, "Effect of flow nonparallelism in a shock layer on a flat plate and the angle of attack on the characteristics of density fluctuations," *Izv. Ross. Akad. Nauk, Mekh. Zhidk. Gaza*, No. 2, 49–55 (1999).